THE JOURNAL OF PHYSICAL CHEMISTRY B

 VOLUME 106, NUMBER 40, OCTOBER 10, 2002

LETTERS

^{14}N Quadrupolar, ^{14}N and ^{15}N Chemical Shift, and $^{14}N-^{1}H$ Dipolar Tensors of Sulfamic Acid

Gerard S. Harbison,*,† Young-Sik Kye,†,‡ Glenn H. Penner,§ Michelle Grandin,§,|| and Martine Monette⊥

Department of Chemistry, University of Nebraska at Lincoln, Lincoln, Nebraska 68588-0304, Department of Chemistry and Biochemistry, University of Guelph, Guelph, Ontario, Canada, and Bruker Spectrospin Canada, 555 Steeles Avenue East, Milton, Ontario, Canada

Received: May 28, 2002; In Final Form: September 2, 2002

A ^{14}N solid-state NMR single crystal study was used to determine the ^{14}N quadrupolar, chemical shift, and $^{14}N-^{1}H$ dipolar tensors of sulfamic acid. The quadrupolar tensor is nearly axially symmetric, with the quasi-unique axis aligned 3° away from the N−S bond. The quadrupole coupling constant of 0.794 MHz is substantially less than the gas-phase value (1.6682 MHz); ab initio calculations show that the difference can be attributed almost entirely to the significantly shorter N−S bond in the solid state. The single crystal study, together with ^{15}N CP/MAS and CP/static experiments, yields an isotropic chemical shift that lies close to its solution value, and a chemical shielding anisotropy of about −80 ppm, and the dipolar couplings are about 10% smaller than computed from the neutron structure, probably because of vibrational averaging. All three tensors are almost collinear. HF, MP2, CI, and DFT(B3LYP) calculations of the nitrogen quadrupole coupling constant and shielding are also reported.

Introduction

Sulfamic acid (NH_3SO_3) is a chimera, a molecule with two natures. On one hand it can be regarded as the adduct of the Lewis base ammonia with the Lewis acid sulfur trioxide; on the other it is the zwitterionic tautomer of sulfuric acid amide:

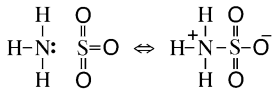

That these two natures are not merely different ways of looking at the chemistry was manifest in the recent publication[1] of the microwave structure of NH_3SO_3. In the gas phase, sulfamic acid is structurally quite markedly different from NH_3-SO_3 in the crystal[2−4] and appears to be much closer to the structure of the Lewis acid adduct than the zwitterion. The gas-phase S−N bond length is 1.9566 Å, considerably greater than the crystal value of 1.7714 Å, and its NSO bond angles of 97.6° put the sulfur trioxide moiety in the gas-phase form more planar and thus closer to its component Lewis acid than the crystal NSO angles of 101.7°, 102.8°, and 102.9°. Microwave spectroscopy also yielded a ^{14}N quadrupole coupling constant (QCC) of −1.69 MHz, intermediate between the −4.09 MHz QCC of free ammonia[5] and the −0.5 to −1 MHz value expected for a $-NH_3^+$ group.[6]

For a molecule of this size, both the gas-phase structure and the QCC should be computable to high accuracy by modern ab initio methods. In 1992, Wong et al.[7] used a self-consistent reaction field model to predict a substantial (0.1 Å) reduction in the N−S bond length in the solid state, compared to the gas phase. The actual reduction is 0.186 Å.

† University of Nebraska Lincoln.
‡ Now at Korea Military Academy, South Korea.
§ University of Guelph.
|| Now at Department of Chemistry, University of Western Ontario.
⊥ Bruker Spectrospin Canada.

10.1021/jp0261962 CCC: $22.00
Published on Web 09/17/2002

The ^{14}N QCC of NH_3SO_3 has unfortunately not been measured in the solid state, and its value, along with the significant structural differences in the solid state, should pose a useful challenge, and test of methods, for incorporating ab initio calculations into crystal lattices. We have therefore undertaken a combined ^{14}N and ^{15}N NMR study of the compound.

Methods

A well-formed single crystal of sulfamic acid, of dimensions approximately 5 mm × 5 mm × 5 mm, was grown from water by slow evaporation and mounted in a Kel-F cell in a singly tuned goniometer probe with the crystal mounted so that the goniometer axis falls in the crystallographic *ab* plane. A home-built NMR spectrometer, operating at 7.187 T (305.9 MHz for ^1H), was used for the ^{14}N single crystal work; data were collected at a temperature of 25 ± 1 °C. All chemical shifts are given relative to liquid ammonia. The ^{14}N chemical shifts were calculated by adding 43.8 ppm to the chemical shift relative to the primary ^{14}N reference signal of crystalline NH_4Cl, which fell at 22.0949 MHz. The chemical shift of crystalline NH_4Cl with respect to liquid ammonia was calculated by assuming that crystalline NH_4Cl has a chemical shift of +14.8 ppm with respect to saturated (5.6 M) NH_4Cl in H_2O[8]; this in turn has a chemical shift of −352.89 ppm relative to external neat nitromethane,[9] which has a shift of +381.93 with respect to liquid ammonia.[9] The ^{14}N 90° pulse length, measured with NH_4Cl, was 4.1 μs; however, because spectra of NH_3SO_3 were often obtained off-resonance with effective irradiation of only a single transition of every pair, a pulse length of 2.5 μs was used.[10] In general, 128 acquisitions were averaged with a recycle delay of 8 s. Because the total spectral width often exceeded the effective spectrometer bandwidth, several spectra were often required to account for all the peaks for each orientation. The peak frequencies were obtained by three-point fits to the peak maxima; typical line widths were 1 kHz. A 180° rotation plot was compiled by recording the resonance frequencies at 7.2° increments.

The ^{15}N spectra were obtained on a Bruker Avance 500 at a frequency of 50.682 MHz using the cross polarization pulse sequence.[11] The 90° pulse was 3.5 μs and a contact time of 7 ms was used. A total of 10 240 acquisitions were acquired, with a recycle delay of 5 s. The ^{15}N NMR signal of crystalline $^{15}NH_4NO_3$ was used as a primary reference; shifts were converted to a liquid NH_3 scale by adding 26.4 ppm.

Calculations employed the programs GAMESS[12] and Gaussian,[13] using standard basis sets (see results). Calculations were done using the HF, MP2, CISD, and DFT methods. Ab initio programs generate electric field gradients in atomic units with actual dimensions of (hartree bohr^{-2}). Quadrupole coupling constants are usually quoted in hertz; they can be straightforwardly calculated from the quadrupole moment Q in square femtometers and the zz element of the electric field tensor $eq = \nabla E_{zz}$ in atomic units, using the conversion factor

$$C_Q = \{((4.35974381 \pm 0.00000034) \times 10^{-18}\ \text{J/hartree}) \times (10^{-15}\ \text{m/fm})^2\}/\{((5.2917720839 \pm 0.0000000019) \times 10^{-11}\ \text{m/bohr})^2((6.62606876 \pm 0.00000052) \times 10^{-34}\ \text{J·s})\} = 2349647.81 \pm 0.26\ \text{Hz hartree}^{-1}\ \text{bohr}^2\ \text{fm}^{-2}$$

and

$$\text{QCC (Hz)} = \nabla E_{zz}\,\text{(au)} \times C_Q \times Q\,(\text{fm}^2)$$

All values of physical constants and their errors are NIST recommended values for 1998.[14] We used the value of the ^{14}N quadrupole moment $Q = 2.05 \pm 0.02$ fm^2 recommended by Cummins et al.[15]

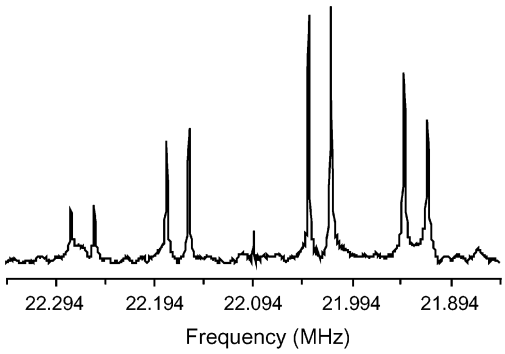

Figure 1. ^{14}N NMR magnitude spectrum of a single crystal of sulfamic acid, obtained as described in the text, at rotation angle $\theta = 100.8°$.

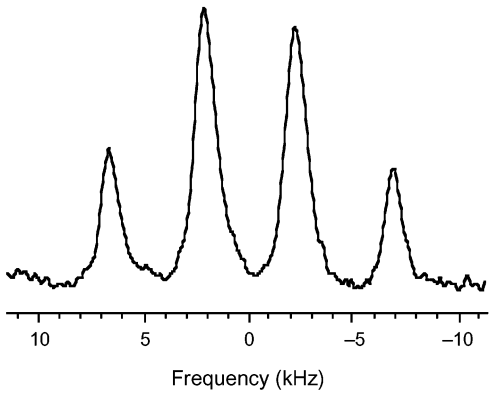

Figure 2. High-frequency region of the ^{14}N NMR spectrum of sulfamic acid, obtained at $\theta = 57.8°$, showing the quartet structure of a molecule with the dipolar unique axis almost parallel to the field.

Chemical shifts with respect to liquid ammonia were obtained from the calculated absolute shielding using the relationship $\delta = 264.5 - \sigma$, all quantities being in parts per million.

Results

Figure 1 shows a rather atypical ^{14}N spectrum of sulfamic acid. The spectrum was collected at an orientation where the sulfamate C_3 axes lie at approximately 50° to the field, and the first-order quadrupolar splittings are therefore rather small. The spectrum shows the eight lines expected from four magnetically inequivalent nitrogens in the unit cell. Line widths are approximately 1 kHz. Because the dipolar and quadrupolar tensors are expected (and found) to be almost collinear, dipolar splittings are also small at this orientation, and the multiplet structure of the resonances falls inside the line width.

At other orientations the spectrum can no longer be obtained in a single spectral window, and the dipolar couplings between the ^{14}N and the proton three-spin system are apparent (see Figure 2). The spectra clearly have the form of a 1:3:3:1 quartet; this, and the magnitude of the splittings, make it clear that the NH_3 protons are in fast exchange between the three sites at room temperature. The frequencies of the lines, or the center-of-gravity of each resolved quartet, are plotted as a function of the rotation angle in Figure 3. The plot has the characteristic pattern of an orthorhombic crystal with three orthogonal 2_1 axes; three "crossings", where the crystallographic *a*, *b*, or *c* axes cross the plane perpendicular to the magnetic field, making the nitrogen resonances pairwise equivalent, can be seen at 0°, 10°, and 95°. The positions of the crossings allow the crystallographic

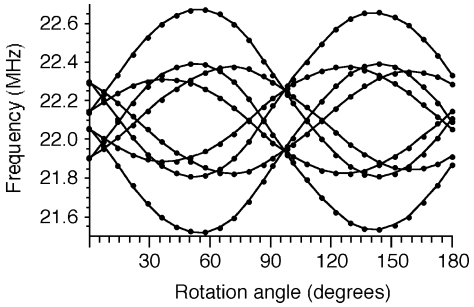

Figure 3. Frequencies of the ^{14}N NMR signals of sulfamic acid as a function of θ. Where resolved quartets were observed, the four quartet frequencies were averaged.

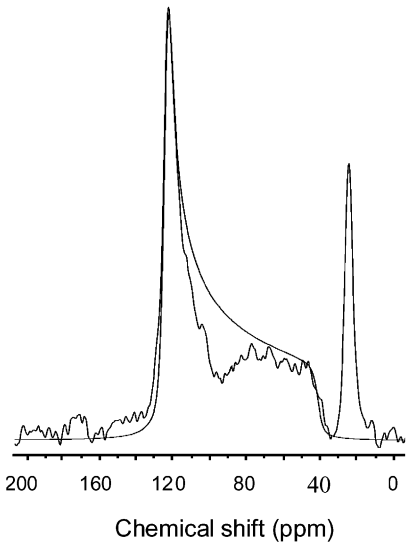

Figure 4. Natural abundance ^{15}N cross-polarization powder spectrum of sulfamic acid, incorporating a small amount of ammonium nitrate as an internal reference.

abc axis system to be located in the goniometer frame of reference, although it is impossible to use symmetry to distinguish which crystallographic axis is which.

The ^{15}N powder spectrum of sulfamic acid (see Figure 4) shows a classic axially symmetric pattern, with a perpendicular edge at 120 ppm and a parallel edge at 45 ppm. The other line in the spectrum is from the ammonium ion in solid ammonium-^{15}N nitrate, used as an internal standard. There appears to be some loss of intensity in the center of the sulfamic acid pattern. This "magic-angle hole" phenomenon is quite frequently observed in the solid-state NMR spectra of materials with comparatively weak heteronuclear dipolar couplings; indeed, it is apparent in spectra of polycrystalline benzene obtained at short contact times, in the seminal work on cross-polarization.[16]

Theory and Data Analysis

^{14}N quadrupolar couplings at fields of the order of 7 T generally are in the second-order regime; that is, the quadrupolar Hamiltonian

$$H_Q = \frac{e^2qQ}{4hI(2I+1)}\left[3I_z^2 - I(I+1) + \frac{\eta}{2}(I_+^2 + I_-^2)\right] \quad (1)$$

is sufficiently large compared with the Zeeman Hamiltonian $H_Z = \gamma B_0 I_z$ that second-order perturbation theory is necessary to fit the transition frequencies accurately. As we have discussed previously,[17] the most straightforward method of data analysis makes use of the fact that the $+1$ and -1 Zeeman eigenstates of the ^{14}N are shifted by the same frequency and with the same sign by the first-order term in the quadrupolar perturbation expansion, and by the same frequency with the opposite sign by the second-order term. Thus, if we add the two observed transition frequencies,

$$\omega_{10} + \omega_{0-1} = E_1 - E_0 - (E_0 - E_{-1}) \quad (2)$$

the sum contains twice the Zeeman frequency, the second-order quadrupolar shift, and twice the chemical shift. If we subtract the two frequencies,

$$\omega_{10} - \omega_{0-1} = E_1 + E_{-1} \quad (3)$$

the result contains only the first-order quadrupolar coupling, which acts like a second-rank tensor, whose *zz* element is the difference of the two transition frequencies. The first-order quadrupole coupling tensor, in its own principal axis frame or PAF, can be written as

$$\mathrm{Q_{PAS}} = \begin{pmatrix} Q_{11} & 0 & 0 \\ 0 & Q_{22} & 0 \\ 0 & 0 & Q_{33} \end{pmatrix} \qquad |Q_{33}| > |Q_{11}| \geq |Q_{22}| \quad (4)$$

where $Q_{33} = 3e^2qQ/2h$ is three-halves of the electric quadrupolar coupling constant, the asymmetry parameter $\eta = (Q_{22} - Q_{11})/Q_{33}$, the tensor is traceless ($Q_{11} + Q_{22} + Q_{33} = 0$), and the sign of the QCC cannot be determined by normal NMR methods. The crystallographic *abc* axis frame (XF) is related to the PAF via the conventionally defined[18] Euler angles α_1, β_1, γ_1 by

$$\mathrm{Q_{XF}} = R(\alpha_1,\beta_1,\gamma_1)Q_{\mathrm{PAF}}R^{-1}(\alpha_1,\beta_1,\gamma_1) \quad (5)$$

As already discussed, there are four molecules in the unit cell, each in its own symmetry frame, We label these frames S0F, S*x*F, S*y*F, S*z*F. The quadrupole tensor in the symmetry frame is

$$Q_{\mathrm{S}n\mathrm{F}} = R_{\mathrm{S}n\mathrm{F}}Q_{\mathrm{XF}}R_{\mathrm{S}n\mathrm{F}}{}^{-1}$$

with

$$R_{\mathrm{S0F}} = \begin{pmatrix} 1 & 0 & 0 \\ 0 & 1 & 0 \\ 0 & 0 & 1 \end{pmatrix} \qquad R_{\mathrm{S}x\mathrm{F}} = \begin{pmatrix} 1 & 0 & 0 \\ 0 & -1 & 0 \\ 0 & 0 & -1 \end{pmatrix}$$

$$R_{\mathrm{S}y\mathrm{F}} = \begin{pmatrix} -1 & 0 & 0 \\ 0 & 1 & 0 \\ 0 & 0 & -1 \end{pmatrix} \qquad R_{\mathrm{S}z\mathrm{F}} = \begin{pmatrix} -1 & 0 & 0 \\ 0 & -1 & 0 \\ 0 & 0 & 1 \end{pmatrix} \quad (6)$$

The quadrupolar tensors in the goniometer frame are obtained from the symmetry frame by rotation about another set of Euler angles

$$Q_{\mathrm{G}n\mathrm{F}} = R(\alpha_2,\beta_2,\gamma_2)Q_{\mathrm{S}n\mathrm{F}}R^{-1}(\alpha_2,\beta_2,\gamma_2) \quad (7)$$

whereas that in the laboratory frame is obtained from the goniometer frame by rotation by an angle θ about the goniometer *x* axis.

$$Q_{\mathrm{L}n\mathrm{F}} = R_{\mathrm{G}}(\theta)Q_{\mathrm{G}n\mathrm{F}}R_{\mathrm{G}}{}^{-1}(\theta)$$

with

$$R_{\mathrm{G}} = \begin{pmatrix} 1 & 0 & 0 \\ 0 & \cos\theta & \sin\theta \\ 0 & -\sin\theta & \cos\theta \end{pmatrix} \quad (8)$$

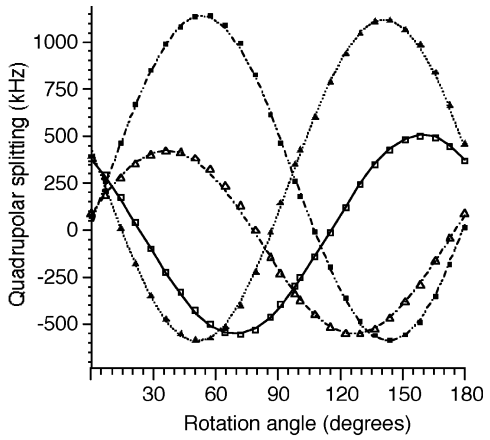

Figure 5. (Points) difference frequencies of the four pairs of quadrupolar doublets; the four sets of symbols identify the four distinct molecules in the unit cell. (Lines) Rotation plots calculated using the quadrupolar tensor determined in this study.

The same analysis can be applied to the chemical shielding and the dipolar interactions, which are much smaller than the quadrupolar interaction and so can be treated entirely adequately by first-order perturbation theory. However, note that the chemical shielding tensor is not traceless. Whereas the chemical shift and dipolar coupling tensors will have their own orientations in the crystallographic frame and thus their own sets of Euler angles α_1, β_1, and γ_1, the other transformations between the crystallographic frame and the laboratory frame are accomplished by the same rotation matrixes in all three cases.

Quadrupolar doublets from the primary rotation plot shown in Figure 3 were identified and sums and differences of each pair taken. The difference plot is shown in Figure 5. As can be seen, the plots intersect pairwise at angles $\theta = 0°$ and 10°. Because this means that two crystallographic axes cross the field almost simultaneously, the third axis must be almost parallel to the field around this orientation. This gives a excellent initial estimate of the orientation of the crystallographic frame relative to the goniometer, with the proviso that the individual *a*, *b*, and *c* axes cannot yet be distinguished. With this preliminary estimate of the Euler angles α_2, β_2, γ_2, an initial guess of an axially symmetric quadrupolar tensor oriented along the N−S bond, and a preliminary estimate of a quadrupolar coupling of 1 MHz, a theoretical rotation plot was calculated, and iteratively fit to the experimental data by a steepest-descents least squares procedure, optimizing the eight parameters Q_{33}, η, α_1, β_1, γ_1, α_2, β_2, and γ_2. The optimum fit is shown by the calculated (solid) curves in Figure 5; the partial derivatives of the variance with respect to each of the parameters were used to factor the residual into variances of each of the parameters. Values ($\pm\sigma$) of $Q_{33} = 1191 \pm 11$ kHz, $\eta = 0.082 \pm 0.054$ were obtained. The value Q_{33} corresponds to the quadrupolar splitting with the unique axis parallel to the field; it equals three-halves the quadrupolar coupling constant, which is therefore 794 ± 8 kHz. The orientation of the crystallographic axis system in the goniometer frame was given by

$$(\alpha_2, \beta_2, \gamma_2) = (90.03 \pm 0.27°, 91.66 \pm 0.34°, 203.02 \pm 0.47°)$$

These errors are smaller than could be obtained by conventional X-ray or optical goniometric crystal alignment, and therefore this orientation was used in subsequent data analysis.

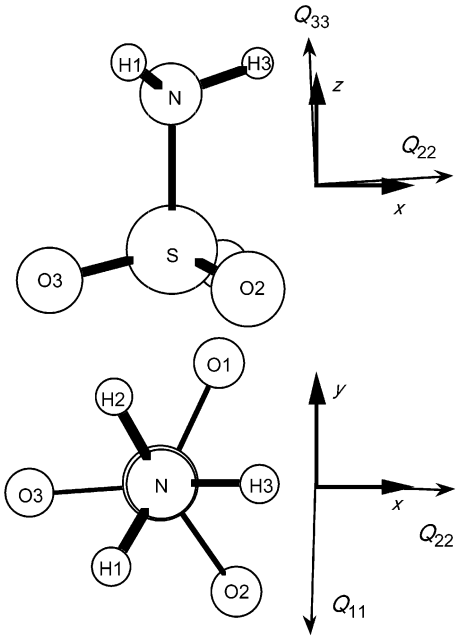

Figure 6. Orientation of the local molecular frame used in this study, relative to atomic positions derived from the low-temperature neutron diffraction structure.[4]

TABLE 1: Direction Cosines of the Local Molecular Frame Used in This Work, Relative to the Crystallographic *abc* Axis System

	a	*b*	*c*
x	0.8177	0.4655	−0.3387
y	0.0033	0.5846	0.8113
z	0.5757	−0.6645	0.4765

TABLE 2: Quadrupolar Tensor Principal Values and Direction Cosines of the Principal Axes in the Crystallographic and the Local Molecular Frame Shown in Figure 4

	freq (kHz)	*a*	*b*	*c*	*x*	*y*	*z*
Q_{11}	−644.2	0.8072	0.4506	−0.3814	0.9978	−0.0251	−0.0619
Q_{22}	−546.8	0.0684	0.5703	0.8186	0.0261	0.9995	0.0157
Q_{33}	1191.0	0.5863	−0.6868	0.4295	0.0615	−0.0172	0.9980

The Euler angles giving the quadrupolar principal axis system in the crystallographic frame were

$$(\alpha_{1Q}, \beta_{1Q}, \gamma_{1Q}) = (-65.10 \pm 5.20°, 115.43 \pm 0.32°, -229.51 \pm 0.27°)$$

Note that the angle α_{1Q}, which governs the orientation of the similar Q_{11} and Q_{22} elements, is much less constrained by the data than the other two angles, which define the orientation of the unique axis; similar effects were seen in the first single crystal determination of a peptide ^{15}N tensor.[19]

To orient the quadrupolar principal axis system relative to the molecule, a local molecular frame was constructed as follows: the *z* axis is parallel to the S−N vector (extracted from the low-temperature neutron structure[4]), the *y* axis lies in the S−N−H(3) plane, and the *x* axis is orthogonal to these two. The orientation of the quadrupolar tensor relative to this axis system is depicted in Figure 6 and given relative to both the local and the crystallographic axis system in Table 2.

Because the quadrupolar tensor was found to be nearly axially symmetric, the asymmetry parameter can be assumed to be zero

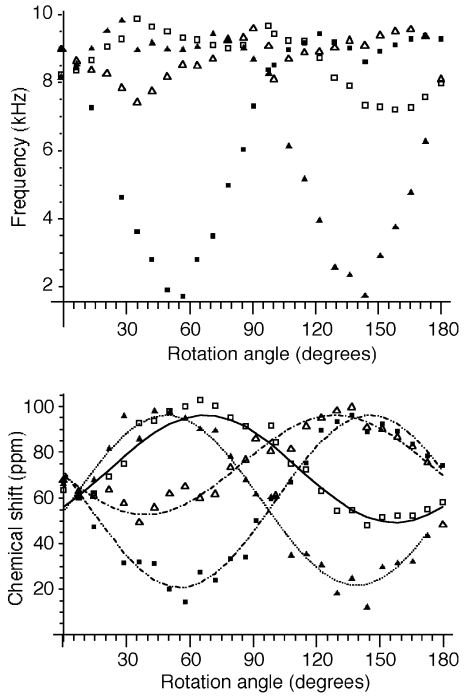

Figure 7. (a) (Top) sum frequencies of the four pairs of quadrupolar doublets; the four sets of symbols identify the four distinct molecules in the unit cell. (b) (Bottom) the same frequencies with the calculated second-order quadrupolar contributions subtracted out, leaving the chemical shift interaction. (Lines) rotation plots calculated using the chemical shift tensor determined in this study.

in the expression for the second-order quadrupolar shift. The shift is then given by the formula

$$\nu_Q^{(2)} = \left(\frac{{Q_{33}}^2}{48\nu_L}\right)(3 + 6\cos^2\theta - 9\cos^4\theta)) \qquad (9)$$

with ν_L as the ^{14}N nuclear Larmor frequency, and θ the angle between the quadrupolar unique axis and the field, which can be extracted from the first-order quadrupolar splitting. This shift was calculated for every point in the rotation plot and subtracted from the sum frequencies, shown at the top of Figure 7. Clear evidence of the second-order shift is seen from the presence of sin 4θ and cos 4θ terms in the plot. Once the second-order shift is subtracted, however, the residual values shown only 2θ dependence, which is assumed to be due to the chemical shift.

These residual sum frequencies were initially fit iteratively in a six-parameter fit to σ_{11}, σ_{22}, σ_{33}, $\alpha_{1\sigma}$, $\beta_{1\sigma}$, $\gamma_{1\sigma}$. However, it was soon apparent that the chemical shift tensor is nearly axially symmetric, and the asymmetry parameter is significantly smaller than the error in its determination. The tensor was therefore constrained to be axially symmetric and fit to an isotropic chemical shift and a chemical shift anisotropy, with the Euler angle $\alpha_{1\sigma}$ omitted as meaningless. The best fit to these quantities gave $\delta_i = 99.7 \pm 2.7$ ppm and $\Delta\delta = 3(\delta_{zz} - \delta_i)/2 = -77.5 \pm 9.1$ ppm. The orientation of the chemical shielding unique axis in the crystallographic frame is given by two angles:

$$(\beta_{1\sigma}, \gamma_{1\sigma}) = (115.9 \pm 4.3°, -226.0 \pm 3.6°)$$

The orientation of the chemical shift tensor relative to the local and the crystallographic axis systems is given in Table 3.

Finally, the observed dipolar splittings (difference between the frequencies of the outer pair of each quartet) were plotted as shown in Figure 8. Though, in principle, hopping between

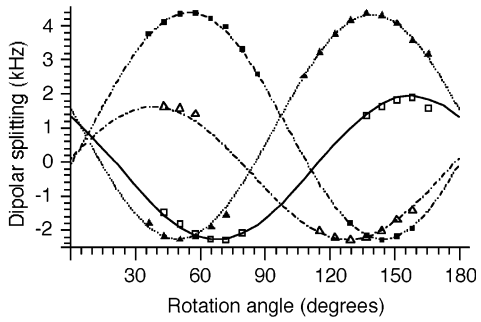

Figure 8. (Points) measured dipolar multiple splittings as a function of the rotation angle. The four sets of symbols identify the four distinct molecules in the unit cell. (Lines) rotation plots calculated using the dipolar tensor determined in this study.

TABLE 3: Chemical Shielding Tensor Principal Values and Direction Cosines of the Unique Principal Axis in the Crystallographic and the Local Molecular Frame Shown in Figure 4[a]

	chemical shift (ppm)	*a*	*b*	*c*	*x*	*y*	*z*
σ_{33}	125.6		undefined			undefined	
σ_{22}	125.6						
σ_{11}	48.0	0.6134	−0.6581	0.4366	0.0474	−0.0286	0.9985

[a] $\sigma_i = 99.7 \pm 2.1$ ppm; $\Delta\sigma = -77.5 \pm 7.1$ ppm.

TABLE 4: Dipolar Tensor Unique Principal Value and Direction Cosines of the Unique Principal Axis in the Crystallographic and the Local Molecular Frame Shown in Figure 4

	freq (Hz)	*a*	*b*	*c*	*x*	*y*	*z*
D_{33}	4564 ± 89	0.6083	−0.6650	0.4332	0.0410	−0.0353	0.9985

slightly non-C_{3v} symmetric positions of the $-NH_3^+$ group might give an axially asymmetric dipolar tensor, as has been observed for deuterium quadrupolar tensors in distorted methyl groups;[20] in practice, the quality of the data did not justify inclusion of an asymmetry parameter, and the data were fit to three parameters; one magnitude and two angles. The value D_{33} corresponds to the splitting between the outer lines of the dipolar quartet with the dipolar unique axis parallel to the field.

$$(D_{33}, \beta_{1D}, \gamma_{1D}) = (4564 \text{ Hz} \pm 89 \text{ Hz}, \beta_{1D} = 115.7 \pm 0.9°, \gamma_{1D} = -226.6 \pm 1.0°)$$

The orientation of the dipolar principal axis relative to the local and the crystallographic axis systems is given in Table 4.

Discussion

It has long been known that crystals with three orthogonal 2-fold screw axes can be fit purely from a single rotation plot and without independent orientation of the crystal. In fact, orienting the crystal by independent means—optical or X-ray—adds no additional information, because the identification of the three symmetry axes located in the single crystal NMR experiment, with the crystallographic *a*, *b*, and *c* axes, is equivalent to the assignment of the four quadrupolar doublets to the four independent molecules in the unit cell. In the present case, this was done by noting the close match of one of the quadrupolar tensors to the molecular N−S axis and confirmed by the orientation of the dipolar tensor, whose orientation is known nearly exactly.

The quadrupolar coupling constant we determine is less than half the magnitude of the gas-phase value of −1.6882

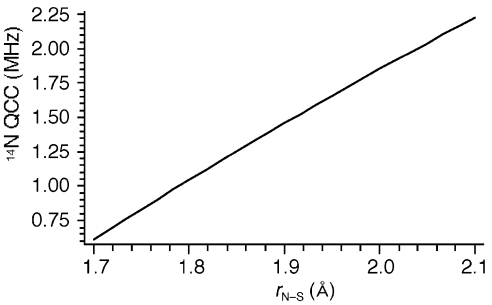

Figure 9. ^{14}N nuclear quadrupolar coupling constant as a function of the N−S bond length, computed as described in the text.

TABLE 5: Computed Dipolar Tensor Principal Values and Direction Cosines of the Principal Axes in the Crystallographic Frame

	freq (kHz)	*a*	*b*	*c*
D_{11}	−2546	−0.5811	−0.7536	−0.3071
D_{22}	−2496	−0.5599	0.0964	0.8229
D_{33}	5042	0.5905	−0.6502	0.4780

TABLE 6: Calculated Nitrogen-14 QCC Values for SO_3NH_3

method/basis set	r_{NS} = 1.771 Å	r_{NS} = 1.957 Å
HF/STO-3G	−2.500	−4.158
HF/6-311++G(d,p)	−1.166	−1.820
MP2/6-311++G(d,p)	−0.939	−1.656
MP2/6-311++G(2d,p)	−0.964	−1.688
CISD/6-31+G(d)	−0.949	−1.542
B3LYP/6-311++G(2d,p)	−0.949	−1.676
experimental value	±0.794[a]	−1.668[b]

[a] This work. [b] Reference 1.

MHz determined by Canargaratna et al.[1] The nonzero asymmetry parameter presumably reflects the structural inequivalence of the three hydrogens, and it is notable that the in-plane direction of the Q_{22} element is toward the most distinct of the three hydrogens. This inequivalence is probably also reflected in the orientation of the quadrupolar principal axis, which is significantly perturbed away from the N−S axis in the same direction.

To examine the source of the substantial difference between gas and solid-phase quadrupole constants, we calculated optimized geometries for sulfamic acid at fixed N−S distances between 1.7 and 2.2 Å, using constrained C_{3v} symmetry. The equilibrium N−S bond length at the MP2/ 6-311G++(2d,p) level of theory (r_e = 2.066 Å; total energy = 679.391 Hartrees) was rather surprisingly divergent from the experimental value of 1.957 ± 0.023 Å, although it was similar to Wong et al.'s[7] MP2 value of 2.081 Å, obtained with a somewhat more limited basis set. The explanation for the divergence probably lies in the extreme softness of the N−S potential. Our calculations show that compressing the N−S bond by 0.1 Å from 2.05 to 1.95 Å and re-optimizing the rest of the structure increases the computed energy by only 235 cm^{-1}. Notably, if r_{N-S} is fixed at 1.957 Å, the optimal NSO bond angle is calculated to be 97.35°, in excellent agreement with the experimental value of 97.6° ± 0.4°.

Figure 9 shows the computed ^{14}N QCC as a function of r_{N-S} for these otherwise optimized structures. The computed ^{14}N QCC at the gas-phase N−S bond length of 1.957 Å is −1.6857 MHz (experiment: −1.6882 ± 0.0054 MHz); at the crystallographic bond length of 1.7714 Å, it drops to −0.9246 MHz. The dependence of the computed QCC at both gas phase and solid-state bond lengths is shown in Table 6. The QCC is a simple function of the ground-state electron density, and the near identity of the results with three different methods of accounting for electron correlation reflects this; Hartree−Fock QCCs are in both cases 10−20% larger. Given the often substantial influence of lattice effects on quadrupolar coupling constants in ionic solids, our computed values are very close to the experimental value of ±0.794 ± 0.008 MHz measured in the present work, although it is within the bounds of possibility that the computed and experimental signs are opposite. If we discount that possibility, it appears that the major reason for the difference between ^{14}N QCCs in the solid and gas phase is simply the difference in N−S bond lengths, with hydrogen-bonding and lattice electrostatic charges responsible for the residual differences.

The chemical shielding tensor is almost collinear with the quadrupolar tensor. The isotropic shift of sulfamic acid in aqueous solution at low pH was measured to be −286.4 ppm relative to a nitrate solution of unspecified composition;[21] converting this to our scale by adding 383.8 ppm,[22] we obtain a solution chemical shift of 97.4 ppm, within experimental error of the ^{14}N NMR value of 99.7 ppm and the ^{15}N MAS value of 95.0 ppm. The agreement between the ^{14}N single crystal data and ^{15}N powder spectrum is gratifyingly good. The chemical shielding anisotropy of sulfamic acid is significantly larger than that of protonated primary amines.[23]

We compare computed and experimental nitrogen shielding tensors in Table 7, as a function of the level of theory. As has often been observed to be the case, the Becke three-parameter functional appears to do an excellent job of accounting for electron correlation in the chemical shielding tensor, athough Hartree−Fock results with a large basis set are also quite close. Curiously, for this system, MP2 deviates markedly from experiment.

The measured dipolar coupling is a function of both the bond lengths and the bond angles within the $-NH_3$ group; because there is no prospect of a unique determination of these values from a single dipolar magnitude and two angles, a direct comparison with a calculated averaged coupling, computed from the low-temperature neutron structure, was felt to be a more useful approach. The computed and experimental dipolar tensors were found to be in excellent agreement if fast exchange between three sites is assumed. In this calculation, dipolar

TABLE 7: Calculated Nitrogen Chemical Shifts and Chemical Shift Anisotropies of SO_3NH_3

	r_{NS} = 1.771 Å		r_{NS} = 1.957 Å	
	δ_i	$\Delta\delta$	δ_i	$\Delta\delta$
HF/STO-3G//HF/STO-3G	−22.0	−27.7	−24.0	−22.1
HF/6-311++G(d,p)//HF/6-311++G(d,p)	100.0	−77.3	85.4	−68.3
MP2/6-31G(d,p)//MP2/6-311++G(d,p)	66.2	−77.8	55.2	−64.9
B3LYP/6-311++G(2d,p)/B3LYP/6-311++G(2d,p)	106.4	−87.6	98.1	−80.0
experimental values	95.0 ± 0.2[a]	−80 ± 5[a]	N/A	N/A
	97.1 ± 2.7[b]	−77.5 ± 7.1[b]		

[a] From ^{15}N CP/MAS and CP/static spectra. [b] From ^{14}N single crystal spectra.

Hamiltonians for the three distinct N−H bonds were averaged in the same frame of reference, and diagonalized, giving the coupling tensor eigenvalues and eigenvectors shown in Table 5. As is the invariable result of vibrational averaging;[24] the experimental dipolar coupling is about 10% less than the value computed from the neutron structure. The computed asymmetry parameter is very small (<0.01), whereas the unique axis is oriented almost exactly along the N−S bond.

One anomaly of the present results for which we are unable yet to provide a good explanation is the consistency in the misalignment of the three tensor unique axes with the N−S bond. All three unique axes lie about 3° from the bond axis, whereas the dipolar and quadrupolar tensor unique principal axes are within 0.8° of each other, and the chemical shift and quadrupolar tensor principal axes are 2.4° apart, probably reflecting experimental error in the determination of the former. The quadrupolar unique axis orientation in particular deviates by several σ from the N−S bond. Although it is possible that this misalignment arises from unaccounted error in the determination of the crystallographic orientation, fixing the quadrupolar axis along N−S and optimizing the crystallographic orientation does not substantially change the crystal alignment or reduce the variance. It is more plausible that the N−S bond vector changes its orientation between 77 K and room temperature; unfortunately, the early room-temperature crystallographic studies[2,3] are insufficiently accurate to test this possibility. And, finally, it is possible that the misalignment is a real phenomenon and reflects the significant distortion of the molecule away from C_{3v} symmetry in the solid state.

Acknowledgment. G.S.H. is grateful for support from the U.S. National Science Foundation (MCB-9605421) and the National Institutes of Health (R01 GM 065252-01). G.H.P. is supported by a grant from the Natural Sciences and Engineering Research Council of Canada.

References and Notes

(1) Canagaratna, M.; Phillips, J. A.; Goodfriend, H.; Leopold, K. R. *J. Am. Chem. Soc.* **1996**, *118*, 5290.
(2) Kanda, F. A.; King, A. J. *J. Am. Chem. Soc.* **1951**, *73*, 2315.
(3) Sass, R. L. *Acta Crystallogr.* **1960**, *13*, 320.
(4) Bats, J. W.; Coppens, P.; Koetzle, T. F. *Acta Crystallogr.* **1977** *B33*, 37.
(5) Hougen, J. T. *J. Chem. Phys.* **1972**, *57*, 4207.
(6) e.g. Blinc, R.; Mali, M.; Osredkar, R.; Prelesnik, A.; Zupancic, I.; Ehrenberg, L. *Chem. Phys. Lett.* **1971**, *9*, 85.
(7) Wong, M. W.; Wiberg, K. B.; Frisch, M. J. *J. Am. Chem. Soc.* **1992**, *114*, 523.
(8) Roberts, J. E.; Harbison, G. S.; Munowitz, M. G.; Herzfeld J.; Griffin, R. G. *J. Am. Chem. Soc.* **1987**, *109*, 4163.
(9) Witanowski, M.; Stefaniak, L.; Szymanski, S.; Januszewski, H. *J. Magn. Reson.* **1977**, *28*, 217.
(10) Man, P. P.; Klinowski, J.; Trokiner, A.; Zanni, H.; Papon, P. *Chem. Phys. Lett.* **1988**, *151*, 143.
(11) Pines, A.; Gibby, M. G.; Waugh, J. S. *J. Chem. Phys.* **1973**, *59*, 569.
(12) Schmidt, M. W.; Baldridge, K. K.; Boatz, J. A.; Elbert, S. T.; Gordon, M. S.; Jensen, J. J.; Koseki, S.; Matsunaga, N.; Nguyen, K. A.; Su, S.; Windus, T. L.; Dupuis, M.; Montgomery, J. A. *J. Comput. Chem.* **1993**, *14*, 1347.
(13) Frisch, M. J.; Trucks, G. W.; Schlegel, H. B.; Scuseria, G. E.; Robb, M. A.; Cheeseman, J. R.; Zakrzewski, V. G.; Montgomery, J. A., Jr.; Stratmann, R. E.; Burant, J. C.; Dapprich, S.; Millam, J. M.; Daniels, A. D.; Kudin, K. N.; Strain, M. C.; Farkas, O.; Tomasi, J.; Barone, V.; Cossi, M.; Cammi, R.; Mennucci, B.; Pomelli, C.; Adamo, C.; Clifford, S.; Ochterski, J.; Petersson, G. A.; Ayala, P. Y.; Cui, Q.; Morokuma, K.; Malick, D. K.; Rabuck, A. D.; Raghavachari, K.; Foresman, J. B.; Cioslowski, J.; Ortiz, J. V.; Stefanov, B. B.; Liu, G.; Liashenko, A.; Piskorz, P.; Komaromi, I.; Gomperts, R.; Martin, R. L.; Fox, D. J.; Keith, T.; Al-Laham, M. A.; Peng, C. Y.; Nanayakkara, A.; Gonzalez, C.; Challacombe, M.; Gill, P. M. W.; Johnson, B. G.; Chen, W.; Wong, M. W.; Andres, J. L.; Head-Gordon, M.; Replogle, E. S.; Pople, J. A. *Gaussian 98*, revision A.7; Gaussian, Inc.: Pittsburgh, PA, 1998.
(14) http://physics.nist.gov/cuu/Constants/index.html.
(15) Cummins, P. L.; Bacskay, G. B.; Hush, N. S.; Ahlrichs, R. *J. Chem. Phys.* **1987**, *86*, 6908.
(16) Pines, A.; Gibby, M. G.; Waugh, J. S. *J. Chem. Phys.* **1973**, *59*, 569.
(17) Subramanian, R.; Koch, S. A.; Harbison, G. S. *J. Phys. Chem.* **1993**, *97*, 8625.
(18) Mehring, M. *Principles of high-resolution NMR in solids*; Springer-Verlag: Berlin and New York, 1983.
(19) Harbison, G. S.; Jelinski, L. W.; Stark, R. E.; Torchia, D. A.; Herzfeld, J.; Griffin, R. G. *J. Magn. Reson.* **1984**, *60*, 79.
(20) Wann, M.-H.; Harbison, G. S. *J. Chem. Phys.* **1994**, *101*, 231.
(21) Naulet, N.; Martin, G. J.; Barieux, J. J.; Combroux, J. F. *J. Chem. Res., Synop.* **1980**, *4*, 158.
(22) Martin, G. J.; Martin, M. L.; Gouesnard, J. P. *^{15}N NMR Spectroscopy*; Springer-Verlag: Berlin, 1981.
(23) Harbison, G. S.; Herzfeld, J.; Griffin, R. G. *J. Am. Chem. Soc.* **1981**, *103*, 4752.
(24) Roberts, J. E.; Harbison, G. S.; Munowitz, M. G.; Herzfeld, J.; Griffin, R. G. *J. Am. Chem. Soc.* **1987**, *109*, 4163.